Journal of Photochemistry and Photobiology A: Chemistry 290 (2014) 22–30

Contents lists available at ScienceDirect

Journal of Photochemistry and Photobiology A: Chemistry

journal homepage: www.elsevier.com/locate/jphotochem

Tunable molecular configuration for significant enhancement of two-photon absorption based on novel octupolar benzoimidazole derivatives

Xingye Zhang [a,c], Zhe Xu [b], Ziyi Ge [a,*], Xinhua Ouyang [a,**], Wei Ji [b,***]

[a] Ningbo Institute of Materials Technology and Engineering (NIMTE), Chinese Academy of Sciences (CAS), Ningbo 315201, PR China
[b] Department of Physics, National University of Singapore, 2 Science Drive 3, Singapore 117542, Republic of Singapore
[c] University of Chinese Academy of Sciences, Beijing 100049, PR China

ARTICLE INFO

Article history:
Received 1 March 2014
Received in revised form 27 May 2014
Accepted 4 June 2014
Available online 11 June 2014

Keywords:
Molecular configuration
Two-photon absorption
Charge transfer performance
Excited-state dipoles

ABSTRACT

Two novel octupolar molecules including benzoimidazole electron-accepting (A) branches and a triphenylamine electron-donating (D) center have been synthesized and characterized (p-ETBN and m-ETBN). Their photophysical and photochemical properties were investigated systematically including single-photon absorption, two-photon absorption (2PA) and charge transfer performance. Their 2PA properties have been investigated by the open aperture Z-scan technique, and the values of the 2PA cross section at 800 nm for p-ETBN and m-ETBN are ~300 GM and ~100 GM, respectively. Interestingly, both of them have the same D, A and π-conjugating units with only the different molecular configuration, the 2PA response of them differs by almost three times, which are found to be the different excited-state dipole moments and intramolecular charge-transfer. Our results reveal a new rule of molecular design for obtaining some excellent 2PA materials for their potential biophotonic and optoelectronic applications.

1. Introduction

Octupolar molecules have been attracting extensively attention owing to their structural symmetry and excellent optical and electronic properties in the past decades [1]. With well-defined structures and suitable conjugated length, they have considerably extended the possibilities of molecular engineering of nonlinear optical molecules by enlarging the dimensionality of the charge transfer [2].

Two-photon absorption (2PA) is a third-order nonlinear optical process involving simultaneous absorption of two low-energy photons to reach the high-energy excited state, which can be applied in many areas including optical limiting [3], two-photon fluorescence excitation microscopy [4], 3D optical data storage [5], two-photon upconversion lasing [3b,6], and photodynamic therapy [7]. Recently, much interest has been focused on the design and synthesis of organic molecules with large 2PA cross sections [8], and theoretical and experimental studies on the relationship between structure and 2PA properties have also been widely investigated [9].

Benzoimidazole-based compounds have been demonstrated showing good electrical and optical properties due to high electron affinity and special structures, which have been extensively used to some fields of optoelectronic devices such as organic field-effect transistors (OFETs), organic light-emitting diodes (OLEDs) and organic photovoltaics (OPVs) [10]. However, up to now, this unit had attracted only scant attention for the nonlinear optical properties. In particular, octupolar molecules consisting of some benzoimidazole electron-accepting (A) branches and an electron-donating (D) center linked through π-conjugated because of the good steric configuration of the conjugated system, strong intramolecular charge-transfer (ICT), and additional cooperative enhancement between the centers [11]. The lack of interest is surprising because, owing to their twisted symmetries, these compounds might exhibit significant nonlinear optical activities when the electron-attracting benzoimidazole branches are symmetrically decorated with the electron-donating centers.

Triphenylamine and their derivatives, as the important electron-donating centers to construct octupolar D–π–A molecules, have attracted great interest owing to their superior electron-donating properties [2d,12]. However, to the best

* Corresponding author.
** Corresponding author. Tel.: +86 574 86686792.
*** Corresponding author.
E-mail addresses: geziyi@nimte.ac.cn (Z. Ge), ouyangxh@nimte.ac.cn (X. Ouyang), phyjiwei@nus.edu.sg (W. Ji).

http://dx.doi.org/10.1016/j.jphotochem.2014.06.002
1010-6030/

of our knowledge, benzoimidazole octupolar molecules using triphenylamine as center, showing enhancement of two-photon absorption with tunable molecular configuration in femotosecond timescales, have still been reported very few during the past decades. Given that such octupolar structures might present good activities for special nonlinear optical properties, we designed and synthesized two isomeric octupolar D–π–A molecules, named p-ETBN and m-ETBN, which contains three benzoimidazole units as branches and one triphenylamine unit as center. Their nonlinear optical properties were studied systematically. It is particularly intriguing to compare the 2PA properties of p-ETBN and m-ETBN, both have the same D, A and π-conjugating units. When changed their molecular configuration, they exhibit an identical 2PA properties, the 2PA response of them differs by almost three times. The DFT computations were conducted to unravel their electronic structures and to rationalize their NOL properties. We wish to modify the photophysical properties of the compounds by changing the molecular configuration and obtain some excellent 2PA materials and to further understand the structure–property relationship.

2. Experimental

2.1. Materials and characterization

Tris(4-bromophenyl)amine, ethynyltrimethylsilane, bis(triphenylphosphine) palladium(II) chloride were purchased from *Tokyo Chemical Industry Co., Ltd*. Cuprous iodide (CuI), dimethyl formamide (DMF), triethylamine (NEt_3) were obtained from J&K Chemical company. All other reagents were from Sinopharm Chemical Reagent Co. Ltd. The solvents were dried using standard procedures. All other reagents were used as received from commercial sources, unless otherwise stated. ^{1}H NMR and ^{13}C NMR spectra were determined in $CDCl_3$ with a Bruker DRX 400 MHz spectrometer. Chemical shifts (*d*) were given relative to tetramethylsilane (TMS). MALDI-TOF mass spectra were recorded on a Shimadzu/Krotos Axima CFR in the linear mode using a laser (λ = 337 nm). Fluorescent and UV–vis spectra of these derivatives were measured with a FLSP920 and HITACHI U3010 spectrophotometers. Tris(4-((trimethylsilyl)ethynyl)phenyl)amine (**1**), tris(4-ethynylphenyl)amine (**2**), 2-(4-bromophenyl)-1-phenyl-1H-benzo[d]imidazole (**3**), and 2-(3-bromophenyl)-1-phenyl-1H-benzo[d]imidazole (**4**) were synthesized following the method reported in the literature [13].

2.2. Synthesis of compound *tris(4-((4-(1-phenyl-1H-benzo[d]imidazol-2-yl)phenyl) ethynyl)phenyl)amine (p-ETBN)*

A 20 mL flask was charged with tris(4-ethynylphenyl)amine **(2)** (0.317 g, 1 mmol), 2-(4-bromophenyl)-1-phenyl-1H-benzo[d]imidazole **(3)** (1.396 g, 4 mmol), PPh_3 (0.104 g, 10%), CuI (0.076 g, 10%) and $Pd(PPh_3)_2Cl_2$ (0.140 g, 5%). The mixture was degassed and backfilled with argon before injecting dried NEt_3 (4 mL) and dried DMF (7.5 mL). The mixture was sealed with a rubber septum and heated to 60 °C for 30 h, then quenched with NH_4Cl and extracted with $CHCl_3$. The organic layer was washed with brine for 2 times and dried over $MgSO_4$ before the solvents was evaporated in vacuum. The residue was purified with column chromatography on silica gel using dichloromethane:hexane (10:1) as eluent to give a yellow solid of **p-ETBN**. Yield: 0.58 g, 52%. ^{1}H NMR (400 MHz, $CDCl_3$): 7.98–7.92 (m, 3H), 7.57 (br, 6H), 7.57–7.54 (m, 9H), 7.46–7.44 (d, 6H, *J* = 7.62 Hz), 7.41–7.39(d, 9H, *J* = 8.50 Hz), 7.34 (br, 9H), 7.27–7.24 (m, 3H), 7.06–7.04 (6H, *J* = 6.07 Hz), ^{13}C NMR (100 MHz, $CDCl_3$): 151.5, 162.5, 146.8, 142.4, 137.1, 136.7, 132.9, 131.4, 130.1, 142.7, 123.8, 123.4, 119.7, 117.7, 110.6, 91.4, 88.9. MALDI-TOF mass: 1122.5 (M^+).

2.3. Synthesis of compound *tris(4-((3-(1-phenyl-1H-benzo[d]imidazol-2-yl)phenyl) ethynyl)phenyl)amine (m-ETBN)*

A 20 mL flask was charged with tris(4-ethynylphenyl)amine **(2)** (0.317 g, 1 mmol), 2-(3-bromophenyl)-1-phenyl-1H-benzo[d]imidazole **(4)** (1.396 g, 4 mmol), PPh_3 (0.104 g, 10%), CuI (0.076 g, 10%) and $Pd(PPh_3)_2Cl_2$ (0.140 g, 5%). The mixture was degassed and backfilled with argon before injecting dried NEt_3 (4 mL) and dried DMF (7.5 mL). The mixture was sealed with a rubber septum and heated to 60 °C for 30 h, then quenched with NH_4Cl and extracted with $CHCl_3$. The organic layer was washed with brine for 2 times and dried over $MgSO_4$ before the solvents was evaporated in vacuum. The residue was purified with column chromatography on silica gel using dichloromethane:hexane (10:1) as eluent to give a yellow solid of m-ETBN. Yield: 3.93 g, 35%. ^{1}H NMR (400 MHz, $CDCl_3$): 7.94–7.90 (t, 6H, *J* = 8.22 Hz), 7.56–7.48 (m, 12H), 7.41–7.27 (m, 12H), 7.35–7.33 (d, 6H, J = 7.00 Hz), 7.32–7.22 (m, 9H), 7.08–7.06 (d, 6H, *J* = 7.87 Hz). ^{13}C NMR (100 MHz, $CDCl_3$): 151.4, 146.7, 142.7, 137.1, 136.6, 132.9, 132.3, 130.2, 129.9, 128.7, 128.2, 127.4, 124.0, 123.6, 123.3, 119.9, 117.7, 90.0, 88.5. MALDI-TOF mass: 1122.2 (M^+).

2.4. Z-scan and pump-probe measurements

The laser pulses were produced by a mode-locked Ti:Sapphire laser (Quantronix, IMRA), which seeded a Ti:Sapphire regenerative amplifier, and focused onto a 1-mm-thick quartz cuvette containing the solutions of the derivatives. The incident and transmitted laser pulse energy were monitored by moving the cuvette along the propagation direction of the laser pulses. The Z-scan experimental system was calibrated using a piece of cadmium sulfide (CdS) bulk crystal as a reference because it possesses large 2PA at the wavelength of 780 nm and has been well investigated in our laboratory. The 2PA coefficient of CdS was determined to be 6.4 ± 0.6 cm GW^{-1}, which was in good agreement with theoretical values within the experiment uncertainty [14].

3. Results and discussions

3.1. Synthesis

Scheme 1 shows the molecular structures and synthetic route of p-ETBN and m-ETBN. It can be seen the molecules contain a triphenylamine center and three benzimidazole branches by linking with the alkynyl groups. Our design of the benzimidazole-type octupolar molecules of p-ETBN and m-ETBN was inspired by the structure of benzimidazole derivatives, a widely used material for fluorescent OLEDs that exhibits high electron mobility and twisted structures. Moreover, the benzimidazole-type octupolar molecules are limited. To expand the family of benzimidazole, a poorly conjugating C≡C is introduced between the benzimidazole and the triphenylamine groups to inhibit the intramolecular charge transfer (ICT), which has been demonstrated to enhance the 2PA [15]. The key intermediate for the synthesis of p-ETBN and m-ETBN was tris(4-ethynylphenyl)amine (**2**), which was synthesized by Sonogashira couplings of tris(4-bromophenyl)amine and ethynyltrimethylsilane using $Pd(PPh_3)_2Cl_2$ and CuI as catalysts. The 2-(4-bromophenyl)-1-phenyl-1H-benzo[d]imidazole (**3**) and 2-(3-bromophenyl)-1-phenyl-1H-benzo[d]imidazole (**4**) were synthesized according to the literature procedures. Further reaction with compounds **2** and **3** or **4** in refluxing dimethyl formamide/triethylamine (15:8, v/v) affords the octupolar molecules

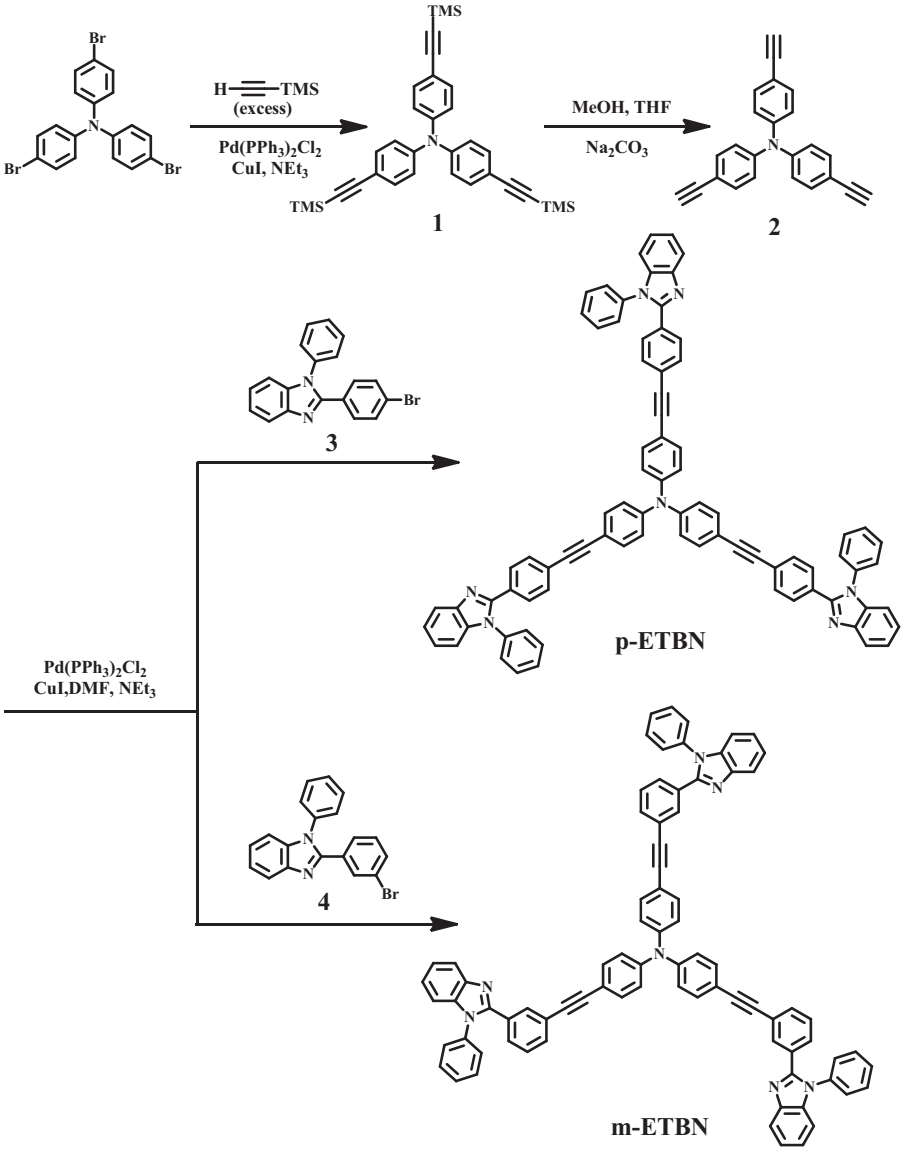

Scheme 1. The synthetic route of octupolar molecules p-ETBN and m-ETBN.

p-ETBN and m-ETBN in suitable yield using Sonogashira conditions. Proton and carbon nuclear magnetic resonance spectroscopy (^{1}H NMR, ^{13}C NMR) and MALDI-TOF were employed to confirm the chemical structures of above-mentioned compounds as described in Section 2.

3.2. UV–vis spectra and electrochemical properties

The normalized UV–vis spectra of the derivatives were measured in chloroform with concentration 2×10^{-5} M as shown in Fig. 1(a). Obviously, p-ETBN and m-ETBN display similar absorptive profiles with two absorptive bands, one is located at ~360–380 nm which assigned to be the transition of π–π^*, another one is about 280–300 nm, which is attribute to the transition of σ–π^*. In the regime of the wavelength of 440–800 nm, they are highly transparent without any absorption. It is clearly shown that the peak of p-ETBN is red shifted by 15 nm than that of m-ETBN, which indicates the fact that the intramolecular charge transfer (ICT) of p-ETBN is larger than that of m-ETBN.

The electrochemical performance of p-ETBN and m-ETBN are studied by cyclic voltammetry in solutions of acetonitrile and THF with a 0.1 M solution of tetrabutylammounium-hexafluorophosphate ($(Bu_4N)PF_6$) as the electrolyte. A Ag/AgCl reference electrode is used as a reference electrode, a Pt disk of 0.01 cm^2 is used as working electrode, and a platinum wire as counter electrode, as shown in Fig. 1(b). The onset oxidation potentials ($E_{onset\text{-}ox}$) for p-ETBN and m-ETBN in acetonitrile are 1.10 V and 1.03 V, respectively, while $E_{onset\text{-}ox}$ for p-ETBN and m-ETBN in THF are 1.11 V and 1.07 V, respectively. The $E_{onset\text{-}ox}$ values obtained from different solvents for the new octupolar molecules are consistent in the range of permitted tolerances. The corresponding HOMO levels for p-ETBN and m-ETBN are determined to be −5.50 eV (−5.51 eV) and −5.43 eV (−5.47 eV), respectively. The band gaps of p-ETBN and m-ETBN can be determined from their onset absorption wavelengths and are calculated to be 2.96 eV and 3.11 eV, respectively, giving corresponding LUMO levels for them of −2.54 eV (2.55 eV) and −2.32 eV (−2.36 eV), individually. In view of this, when these molecules are excited by the wavelength of 700–800 nm, the corresponding p-ETBN and m-ETBN will Exhibit 2PA or 2PEA processes owing to their energy gaps at the range of λ_{exc} to $2\lambda_{exc}$. The photophysical and electrochemical parameters of them are listed in Table 1.

Table 1
The photophysical and electrochemical properties of p-ETBN and m-ETBN.

	λ_{abs} (nm)[a]	ε ($\times 10^4$ M^{-1} cm^{-1})[b]	HOMO/LUMO[c]	HOMO/LUMO[d]	μ_e (D)[e,f]
p-ETBN	400	2.18	−5.50(−5.51)/−2.54(−2.55)	−4.57/−2.59	27.8/4.47
m-ETBN	370	2.75	−5.43(−5.47)/−2.32(−2.36)	−4.64/−2.43	15.3/2.35

[a] Linear absorption peak measured in THF.
[b] Molar absorptivity.
[c] HOMO was estimated based on cyclic-voltammetry (CV) data in acetonitrile and THF; LOMO was deduced from HOMO and optical gaps.
[d] HOMO and LUMO estimated by DFT predications.
[e] Molecular dipole moment of the fluorescent states estimated by Lippert–Matage equation.
[f] Molecular dipole moment estimated by DFT predications.

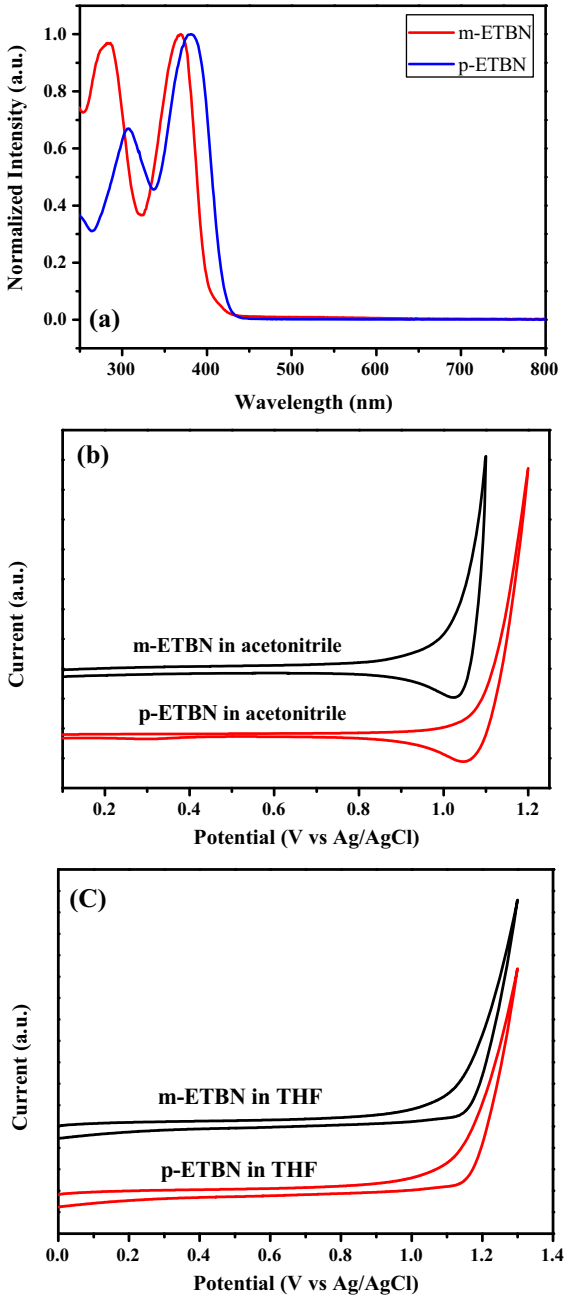

Fig. 1. (a) UV–vis spectra and cyclic voltammograms of p-ETBN and m-ETBN (b) in acetonitrile (c) and in THF.

3.3. Dipole moments

The Solvent effect is usually observed for molecules with a D–π–A structure. So the solvent effect behavior was investigated to evaluate the effect of solvent polarity and excited-states of these molecules (Fig. 2). The emission spectra of p-ETBN and m-ETBN were recorded in different solvents by increasing polarity from petroleum ether to methanol (MeOH). Obviously, as the increase of the solvent polarity, the fluorescence spectra of them exhibit a larger red-shifted and broader shape. Interestingly, for the m-ETBN, a slight solvatochromism is observed in the emission by featuring *meta*-position substituent, whereas a larger and overall positive solvatochromism is observed in the compound p-ETBN for the *para*-position substituent. It can be seen that a large difference in the dipole moment between the excited state and the ground state of them, the CT state with a large polarity is usually stabilized in polar solvents, and the change is consistent with a variety of the excited state from the local excited (LE) state to an excited state with the strong CT character [16]. The dipole moment (μ_e) of the fluorescent states can be estimated from the energies of the fluorescence

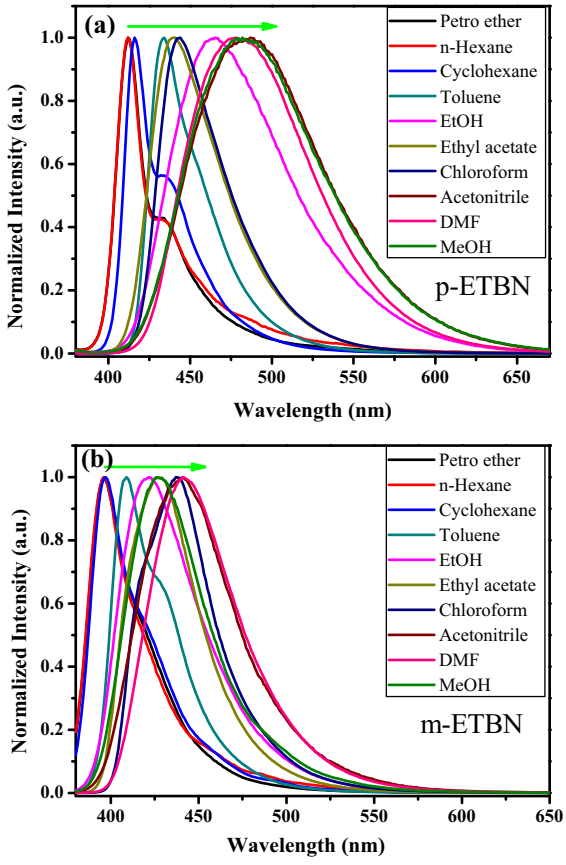

Fig. 2. Fluorescence spectra of p-ETBN and m-ETBN in various polarity solvents.

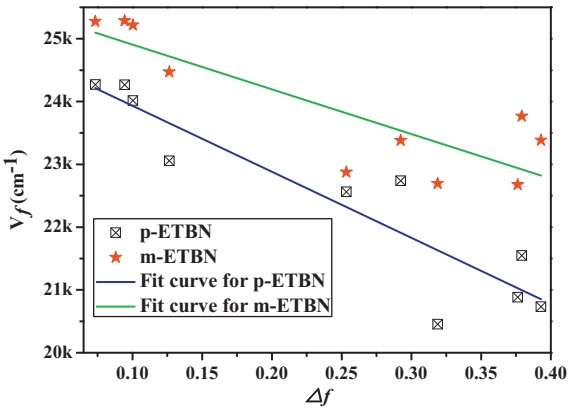

Fig. 3. Solvent polarity (Δf) dependence of the fluorescence maxima of p-ETBN and m-ETBN.

maxima (v_f) against the solvent parameter Δf (shown in Fig. 3 and Table 1) and the values of them are 27.8 D for p-ETBN and 15.3 D for m-ETBN according to the equation of Lippert–Matage [16,17], respectively. Apparently, the large dipole moments of p-ETBN and m-ETBN are one of evidences for the formation of the twisted intramolecular charge transfer state (TICT state). Furthermore, the value of μ_e for p-ETBN is larger than that of the compound m-ETBN, which indicates the charge-transfer of p-ETBN is better than that of m-ETBN. Additionally, by contrasting the emission of p-ETBN and m-ETBN in nonpolar solvent which is from the local excitons, we can found the shoulder peak in p-ETBN is stronger than that of m-ETBN. Likewise, when the excitons change from TICT to LE, the charge-transfer of p-ETBN is also better than that of m-ETBN, it will also enhance the nonlinear absorption. The dipole moments of excited-states were deduced by the formula as following:

$$v_f = \frac{2\mu_e(\mu_e - \mu_g)}{4\pi\varepsilon_0 hca^3}\Delta f + C \quad (1)$$

$$\Delta f = \frac{\varepsilon - 1}{2\varepsilon + 1} - \frac{0.5(n^2 - 1)}{2n^2 + 1} \quad (2)$$

$$a = \left(\frac{3M}{4N\pi d}\right)^{\frac{1}{3}} \quad (3)$$

where μ_g is the ground-state dipole moment, a is the solvent cavity (Onsager) radius, which was derived from Avogadro's number (N), molecular weight (M), and density ($d = 1$), and ε, ε_0, and n are the solvent dielectric constant, vacuum permittivity, and solvent refractive index, respectively. The value of μ_g was calculated at the DFT (density functional theory) model of a DMol3 package in Materials Studio.

3.4. Two-photon absorption properties

In the present study, two-photon absorption (2PA) properties of p-ETBN and m-ETBN dissolved in THF were investigated with femtosecond Z-scans measurements at 780, 800 and 820 nm. To correlate the 2PA data with the results of energy dependent nonlinear transmission studies, a relatively high energy power source at 250 GW cm^2 was applied. However, high laser-pulse irradiation of solutions has been reported to cause thermally induced scattering effects and 2PA induced excited-states absorption. Therefore, in the present study, the measured 2PA cross-section values of p-ETBN and m-ETBN using a relative low laser power. To prevent much deviation of measured 2PA cross-section values from intrinsic two-photon absorptions, effort was taken to reduce accumulative thermal effects to a possibly low level and to minimize the contribution of triplet–triplet state absorption in these molecules by

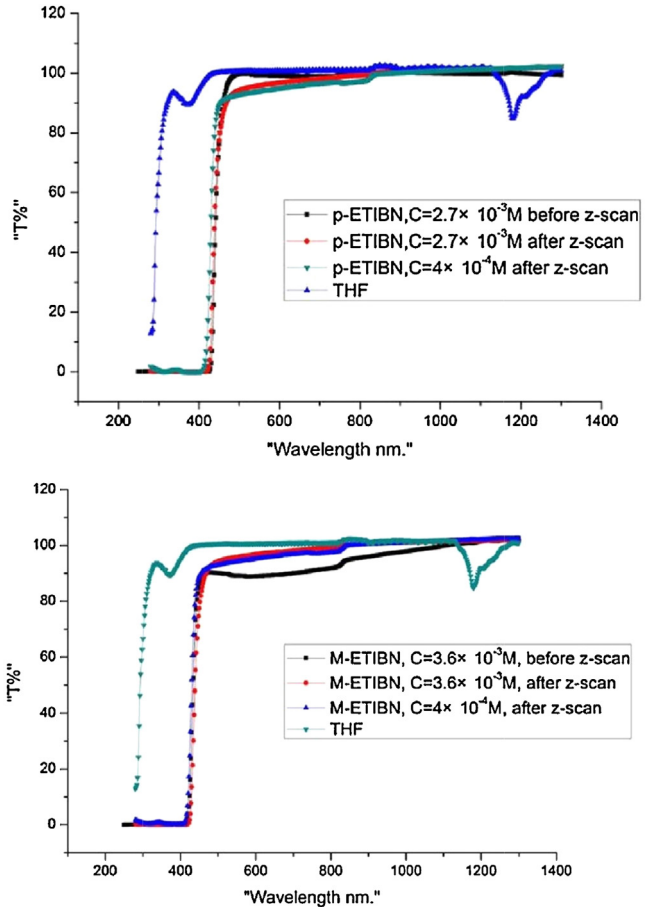

Fig. 4. Transmittance spectra of (a) p-ETBN and (b) m-ETBN.

employing ultrafast 150 fs laser pulses at 1 kHz repetition rate. Prior to 2PA measurements, the concentrations of all ETBN solutions in THF were adjusted to 2–4 × 10^{-3} M and 4 × 10^{-4} M which gives a linear (or low-fluency) transmittance (T) of >90% for all samples at 800 nm, as shown in Fig. 4. The other wavelength (780 and 820 nm) is also shown the high transmittance (T) of >90%.

Firstly, the optimized wavelength of laser is done, we choose the concentration of 10^{-3} M of p-ETBN and m-ETBN to checked, the values of p-ETBN in 780 nm 800 nm and 820 nm are 230 GM, 240 GM and 240 GM, respectively, while the values of m-ETBN are 100 GM, 100 GM and 70 GM. According to the results, we chose the 800 nm wavelength to research the 2PA cross section of ETBN. The nonlinear absorption (NLA) results of p-ETBN and m-ETBN with the different concentrations by the Z-scan measurement technique were shown in Fig. 5a and summarized in Table 2. It can be seen that all Z-scans display a symmetric valley with respect to the focus, typical of an induced positive NLA effect. By fitting the trances of Z-scan theories by two-photon theory [18], we obtain the nonlinear absorption coefficient β (2PA) at different levels of I_{00}. And their nonlinear absorption cross-sections (σ_2) are calculated from the equations of $\sigma_2 = \beta\hbar\omega/n$, respectively, where $\hbar\omega$ is the photon energy and N is the molecular concentration. Unfortunately, for the concentration of 10^{-4} M and pure THF at 800 nm as shown in Fig. 5b, the normalized $\Delta T/T_0$ is found to be less than 5%, which means no TPA exist here.

The measurement of Z-scans of p-ETBN in THF with the concentration of 10^{-3} M at different irradiances are shown in Fig. 6a, and the resulting 2PA cross-section values are potted in Fig. 6b. The results of m-ETBN exhibited similar profiles. Interestingly, the 2PA cross-section values keep almost constant with the different

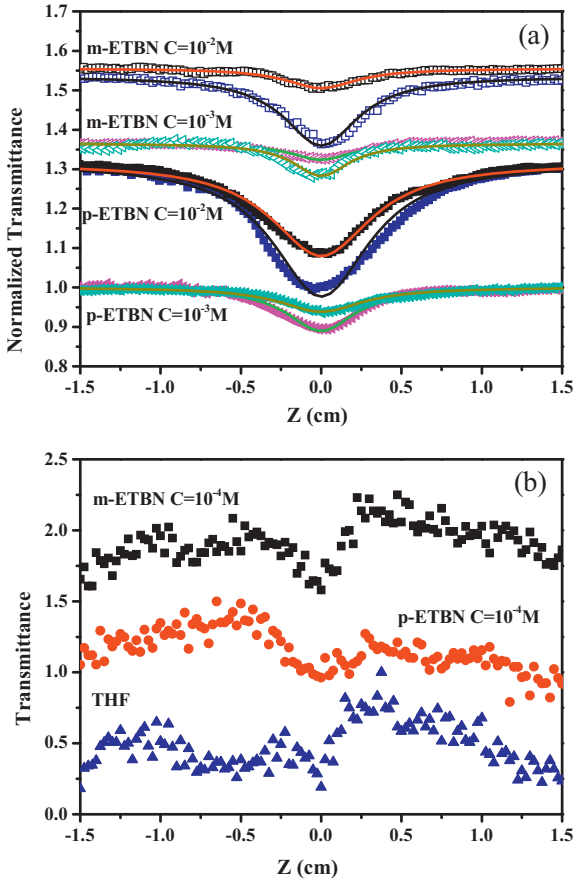

Fig. 5. The Z-scan trance and fitting curve of p-ETBN, m-ETBN and THF.

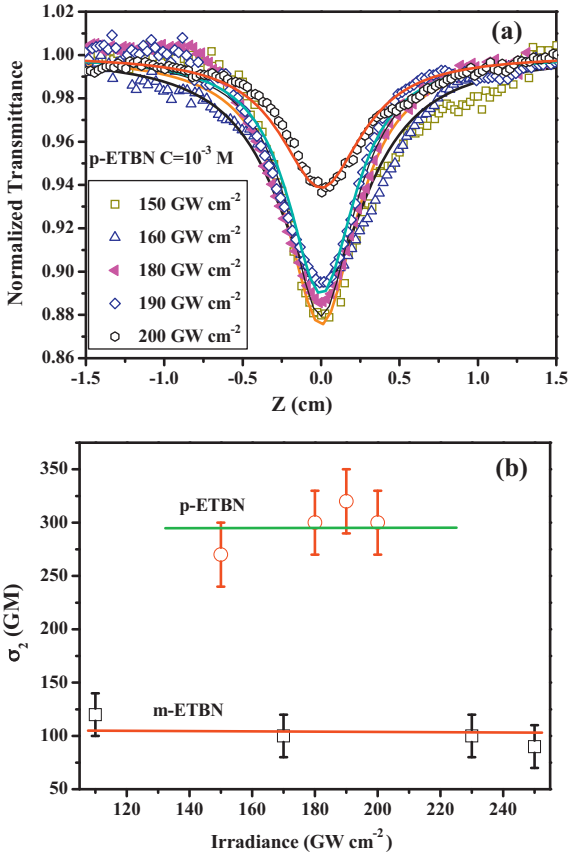

Fig. 6. (a) Open-aperture Z-scans at different excitation irradiances for p-ETBN with experimental data presented as scatter graphs and fitting curves, and (b) irradiance independence of the σ_2 profile of p-ETBN and m-ETBN.

irradiance. It can be confirmed the present NLA is from pure 2PA processes. In the comparison of σ_2 values between p-ETBN and m-ETBN collected at 10^{-3} M concentration, a consistent reduction of the transmittance is found that a larger 2PA coefficient of p-ETBN than that of m-ETBN. Accordingly, an increase of 2PA cross-sections are observed about three times in p-ETBN with their corresponding σ_2 values of m-ETBN, revealed clearly the charge-transfer abilities and excitons change from TICT to LE in p-ETBN lead to a large enhancement of the 2PA. Additionally, we also observed an increase of 2PA cross-sections of ETBN molecules in a consistent trend upon decreasing the solution concentration from 10^{-2} M to 10^{-3} M in THF. The 2PA cross-sections for p-ETBN and m-ETBN at 10^{-2} M were reported with values of ~160 GM and ~50 GM, respectively. When the concentrations of ETBN reduce to 10^{-3} M, the corresponding 2PA cross-sections increase to ~300 GM for p-ETBN and ~100 GM for m-ETBN. The results have been demonstrated by the effect of the molecular aggregation [19].

Table 2
Two-photon absorption cross-section values of p-ETBN and m-ETBN in different concentrations and laser power intensities, measured at 800 nm with 150 fs laser pulses.

	[C] M	I_{00} (GW cm^{-2})	β (cm GW^{-1})	σ_2 (GM)
p-ETBN	1.4×10^{-2}	80	0.054	160
	1.4×10^{-2}	110	0.058	170
	1.4×10^{-2}	120	0.055	160
	1.4×10^{-2}	130	0.059	170
	1.4×10^{-2}	140	0.050	150
	1.4×10^{-2}	150	0.053	160
	1.4×10^{-2}	170	0.065	180
	2.7×10^{-3}	150	0.018	270
	2.7×10^{-3}	160	0.018	270
	2.7×10^{-3}	180	0.020	300
	2.7×10^{-3}	190	0.021	320
	2.7×10^{-3}	200	0.020	300
m-ETBN	1.0×10^{-2}	80	0.014	60
	1.0×10^{-2}	90	0.015	60
	1.0×10^{-2}	130	0.011	40
	1.0×10^{-2}	140	0.012	50
	1.0×10^{-2}	160	0.013	50
	1.0×10^{-2}	200	0.016	60
	1.0×10^{-2}	210	0.015	60
	3.6×10^{-3}	110	0.010	120
	3.6×10^{-3}	170	0.009	100
	3.6×10^{-3}	230	0.009	100
	3.6×10^{-3}	250	0.008	90

3.5. Theoretic predications

To further understand the variation of the photophysical properties of p-ETBN and m-ETBN, especially how the configuration affect the HOMO, LUMO and energy band gaps, their molecular configuration and frontier molecular orbitals and geometrical structures were optimized by using the DFT (density functional theory) model of a DMol3 package in Materials Studio (version 5.5). Atomic basis sets were applied numerically in terms of a double numerical plus polarization (DNP) function (including a polarized d-function for all non-hydrogen atoms and p-function for all hydrogen atoms and a global orbital cutoff of 4.4 Å was employed [20]. The size of the DNP basis set is comparable to Gaussian 6-31G(d), but the DNP is more accurate than the corresponding Gaussian basis set [21]. The exchange–correlation interaction was treated within the generalized gradient approximation (GGA) with the functional parameterized by Perdew, Burke and Enzerhof

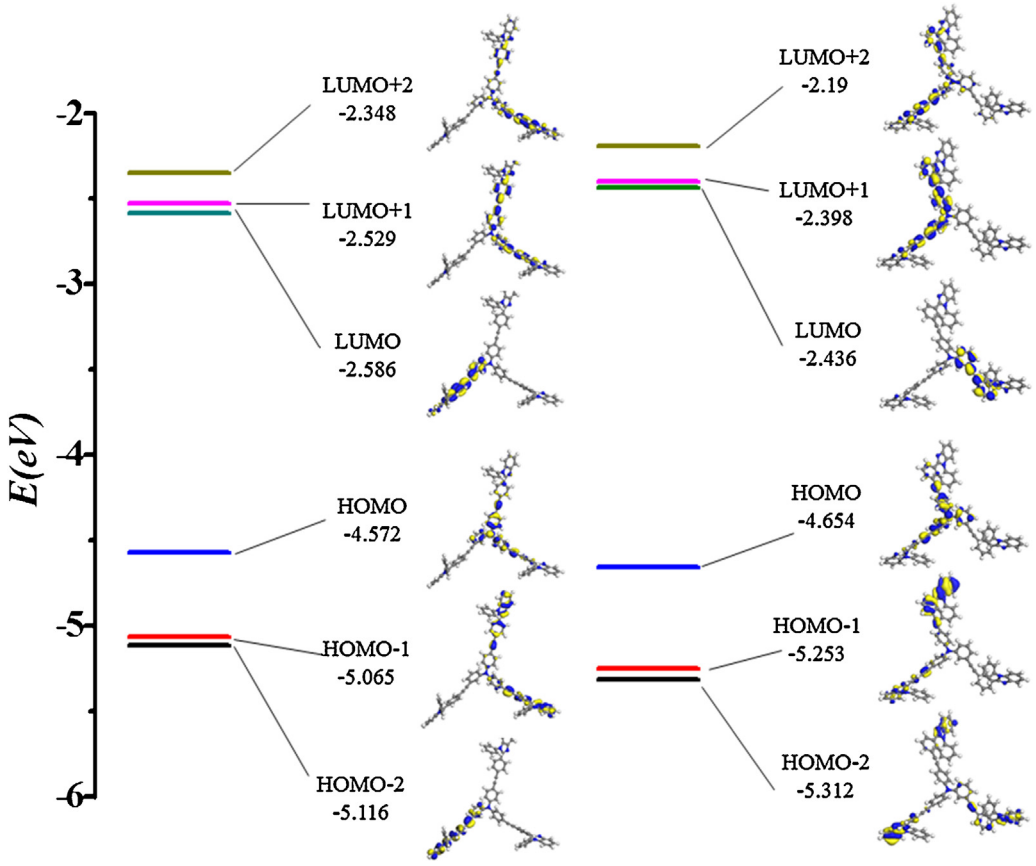

Fig. 7. Spatial distributions of MOs. of p-ETBN and m-ETBN.

(PBE) [22]. The spin-polarization effects were also included in the calculations for the open-shell systems. In contrast to electrochemical analysis, DFT calculations were performed assuming that the complex is in gaseous phase, so that the interaction between the complex and the solvent molecules can be eliminated.

The HOMOs and LUMOs of p-ETBN and m-ETBN were shown in Fig. 7. A large dihedral angle (∼70°) between the N-substituted benzene and benzimidazole planes, this might prevent intramolecular extending of π-electron and suppress molecular packing in the solid state effectively. In addition, these molecules also show the dihedral angles between the triphenylamine moieties and benzimidazole planes with the twisting angles. As expected from the overall symmetry of these molecules, the dipole moment in their ground state is in the range 2–5 D as summarized in Table 1, the large the dipole moments of them indicate these molecules rotate out-of-plane during the optimization procedure. In contrast, the dipole moment of p-ETBN is about two times larger than that of m-ETBN, it can be shown the TICT and LE states in p-ETBN are more active than that of m-ETBN, which is good agreement with the above-discussed about the excited-states of them. The HOMOs of p-ETBN and m-ETBN are essentially located on the triphylamine center, while in LUMO, the π-electrons delocalized on the one benzimidazole branch and partial triphylamine center for p-ETBN. The incomplete separation shows simultaneously existing CT transition of HOMO (donor)→LUMO (acceptor) and LE in these molecules. HOMO-1 and HOMO-2 are nearly degenerate in energy and can be identified with two sister MOs. The energies of HOMO and LUMO are predicated by DFT and summarized in Table 1. It is noted that there are some changes in energies of HOMO and LUMO with the experiments. This may be induced by the interaction between molecules and solvents. In the results of calculation, we only consider the molecules with ideal conditions. And the gradual decrease of values in LUMO is good agreement with the experimental results.

In order to deep investigate the LE and TICT, the relative calculations about their excited-states containing three kinds of solvents (cyclohexane, dichloromethane, methanol) were performed. The dipole moments of ETBN were summarized in Table 3. On the other hand, the important changes containing distances (Å) and dihedral angles (°) of D–A units in ground/excited-state molecules, were shown in Table 4, and the important changes of dihedral angles between the ground- and excited-states of them are shown in Fig. 8. There are obvious differences for molecular conformation between ground states and excited states. Obviously, when we optimized the excited-states of ETBN with the solvent of cyclohexane, the dipole moments of ETBN are 4.98 D (p-ETBN) and 4.42 D (m-ETBN), respectively. The low values are close to the values of their ground states, which can be attributed the local excited states. While performed calculation with methanol, we can find that the dipole moments of ETBN are 29.42 D (p-ETBN) and 18.57 D (m-ETBN), respectively. The large values of them can be assigned from TICT, which is good agreement with experimental results and the published paper of Ouyang et al. [18b] On the other hand, we also optimized the excited-states

Table 3
The calculated dipole moments of ETBN in ground states and excited-states (cyclohexane, dichloromethane and methanol).

Comp.	Dipole moment (ground states)	Dipole moment (excited-states)		
		Cyclohexane	Dichloromethane	Methanol
p-ETBN	4.47	4.98	15.41	29.42
m-ETBN	2.35	4.42	10.78	18.57

Table 4
The important parameters containing distances (Å) and dihedral angles of them on ground- and exited-states.

	Ground states		Exited states	
	p-ETBN	m-ETBN	p-ETBN	m-ETBN
r (7, 8) (Å)	1.4342	1.4212	1.4525	1.4412
r (14, 22) (Å)	1.4401	1.4385	1.4522	1.4423
r (22, 25) (Å)	1.2894	1.2917	1.3011	1.3078
r (25, 48) (Å)	1.3988	1.4191	1.4082	1.4136
Φ (8, 7, 10, 11) (°)	81.9	79.8	82.1	81.7
Φ (55, 56, 60, 88) (°)	−1.4	−1.2	−0.71	−0.95
Φ (77, 75, 82,83) (°)	−111.2	−107.2	−92.3	−97.3
Φ (60, 75, 82, 85) (°)	−144.1	−132.4	−89.3	−92.6

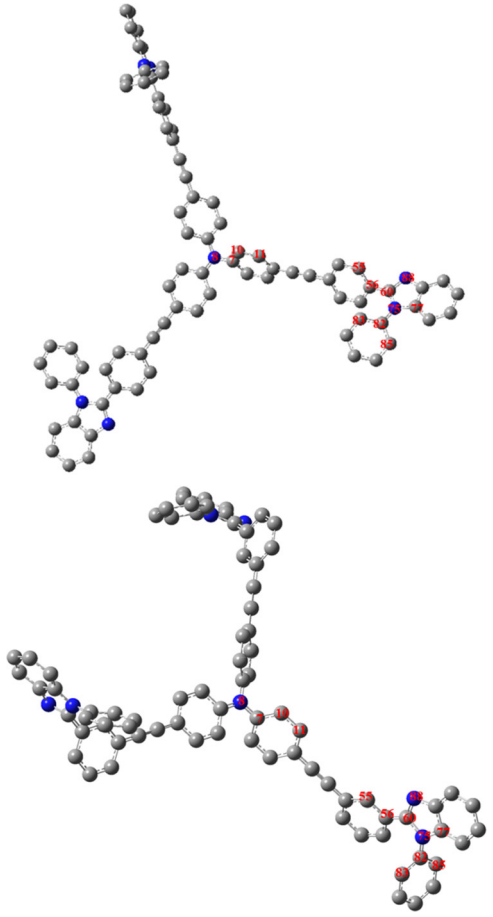

Fig. 8. The important the dihedral angles with the difference between the ground- and excited-states of p-ETBN and m-ETBN.

of them with dichloromethane, the values of them are 15.41 D (p-ETBN) and 10.78 D (m-ETBN). Moreover, we can easily find that the values of p-ETBN with different solvents are all larger than that of m-ETBN. It can be concluded that the charge-transfer of p-ETBN is better than that of m-ETBN, which is agreement with the results of experimental results.

4. Conclusion

In this work, we have successfully demonstrated two novel isomers of p-ETBN and m-ETBN to enhance 2PA by changing their molecular configurations. The value of the 2PA cross section for p-ETBN is three times larger than that of m-ETBN. Their excited-state dipoles and intramolecular charge-transfer performance were studies by solvatochromism and DFT calculation. The results are found that the difference is attributed to the different excited-state dipole moments and intramolecular charge-transfers. Our results reveal a new rule of molecular design for obtaining some excellent 2PA materials for their potential biophotonic and optoelectronic applications.

Acknowledgements

This work was Financial supported from National Natural Science Foundation of China (21074144, 21102156, 51273209), Ningbo International Cooperation Foundation (2012D10009, 2013D10013), the Open Fund of the State Key Laboratory of Luminescent Materials and Devices (South China University of Technology) and the External Cooperation Program of the Chinese Academy of Sciences (No. GJHZ1219). The authors are also thankful to Prof. Yanping Huo, Faculty of Chemical Technology and Light Industry, Guangdong University of Technology, Guangzhou, for supplying the Materials Studio software package.

References

[1] (a) C. Dhenacut, I. Ledoux, I.D.W. SamuelA, J. Zyss, M. Bourgault, H. Lebozec, Chiral metal complexes with large octupolar optical nonlinearities, Nature 374 (1995) 339–342;
(b) W.B. Lin, Z.Y. Wang, L. Ma, A novel octupolar metal–organic NLO material based on a chiral 2D coordination network, J. Am. Chem. Soc. 121 (1999) 11249–11250;
(c) W.H. Lee, H. Lee, J.A. Kim, J.H. Choi, M.H. Cho, S.J. Jeon, B.R. Cho, Two-photon absorption and nonlinear optical properties of octupolar molecules, J. Am. Chem. Soc. 123 (2001) 10658–10667;
(d) Y. Liu, X. Xu, F.K. Zheng, Y. Cui, Chiral octupolar metal–organoboron NLO frameworks with (14,3) topology, Angew. Chem. Int. 47 (2008) 4538–4541;
(e) H.P. Zhou, X. Zhao, T.H. Huang, R. Lu, H.Z. Zhang, X.H. Qi, P.C. Xue, X.L. Liu, X.F. Zhang, Synthesis of star-shaped monodisperse oligo(9,9-di-n-octylfluorene-2,7-vinylene)s functionalized truxenes with two-photon absorption properties, Org. Biomol. Chem. 9 (2011) 1600–1607.
[2] (a) O. Maury, H. Le Bozec, Molecular engineering of octupolar NLO molecules and materials based on bipyridyl metal complexes, Acc. Chem. Res. 38 (2005) 691–704;
(b) D. Beljonne, W. Wenseleers, E. Zojer, Z.G. Shuai, H. Vogel, S.J.K. Pond, J.W. Perry, S.R. Marder, J.L. Bredas, Role of dimensionality on the two-photon absorption response of conjugated molecules: the case of octupolar compounds, Adv. Funct. Mater. 12 (2002) 631–641;
(c) S. Brasselet, F. Cherioux, P. Audebert, J. Zyss, New octupolar star-shaped structures for quadratic nonlinear optics, Chem. Mater. 11 (1999) 1915–1920;
(d) L. Porres, O. Mongin, C. Katan, M. Charlot, T. Pons, J. Mertz, M. Blanchard-Desce, Enhanced two-photon absorption with novel octupolar propeller-shaped fluorophores derived from triphenylamine, Org. Lett. 6 (2004) 47–50;
(e) X.T. Liu, J.F. Guo, A.M. Ren, Z. Xu, S. Huang, J.K. Feng, Theoretical insight into linear optical and two-photon absorption properties for a series of N-arylpyrrole-based dyes, Org. Biomol. Chem. 10 (2012) 7527–7535.
[3] (a) J.E. Ehrlich, X.L. Wu, I.Y.S. Lee, Z.Y. Hu, H. Rockel, S.R. Marder, J.W. Perry, Two-photon absorption and broadband optical limiting with bis-donor stilbenes, Org. Lett. 22 (1997) 1843–1845;
(b) S.L. Oliveira, D.S. Correa, L. Misoguti, C.J.L. Constantino, R.F. Aroca, S.C. Zilio, C.R. Mendonca, Two-photon absorption properties of proquinoidal D–A–D and A–D–A quadrupolar chromophores, Adv. Funct. Mater. 17 (2005) 1890–1893;
(c) S. Jeon, J. Haley, J. Flikkema, V. Nalla, M. Wang, M. Sfeir, L.S. Tan, T. Cooper, W. Ji, M.R. Hamblin, L.Y. Chiang, Linear and nonlinear optical properties of photoresponsive [60]Fullerene hybrid triads and tetrads with dual NIR two-photon absorption characteristics, J. Phys. Chem. C 117 (2013) 17186–17195.
[4] (a) F. Helmchen, W. Denk, Deep tissue two-photon microscopy, Nature 2 (2005) 932–940;

(b) P.T.C. So, C.Y. Dong, B.R. Masters, K.M. Berland, Two-photon excitation fluorescence microscopy, Annu. Rev. Biomed. Eng. 2 (2000) 399–429.
[5] (a) D.A. Parthenopoulos, P.M. Rentzepis, Three-dimensional optical storage memory, Science 245 (1989) 843–845;
(b) N.S. Makarov, A. Rebane, M. Drobizhev, H. Wolleb, H. Spahni, Optimizing two-photon absorption for volumetric optical data storage, J. Opt. Soc. Am. B 24 (2007) 1874–1885.
[6] G.S. He, L.X. Yuan, P.N. Prasad, A. Abbotto, A. Facchetti, G.A. Pagani, Two-photon pumped frequency-upconversion lasing of a new blue-green dye material, Opt. Commun. 140 (1997) 49–52.
[7] (a) J. Arnbjerg, A. Jimenez-Banzo, M.J. Paterson, S. Nonell, J.I. Borrell, O. Christiansen, P.R. Ogilby, Two-photon absorption in the tetraphenyl porphycenes: are porphycenes better candidates than porphyrins for providing optimal optical properties for two-photon photodynamic therapy? J. Am. Chem. Soc. 129 (2007) 5188–5199;
(b) K. Ogawa, H. Hasegawa, Y. Inaba, Y. Kobuke, H. Inouye, Y. Kanemitsu, E. Kohno, T. Hirano, S. Ogura, I. Okura, Water-soluble bis(imidazolylporphyrin) self-assemblies with large two-photon absorption cross sections as potential agents for photodynamic therapy, J. Med. Chem. 49 (2006) 2276–2283;
(c) M.K. Kuimova, H.A. Collins, M. Balaz, E. Dahlstedt, J.A. Levitt, N. Sergent, K. Suhling, M. Drobizhev, N.S. Makarov, A. Rebane, H.L. Anderson, D. Phillips, Photophysical properties and intracellular imaging of water-soluble porphyrin dimers for two-photon excited photodynamic therapy, Org. Biomol. Chem. 7 (2009) 889–896.
[8] (a) M. Albota, D. Beljonne, J.L. Bredas, J.E. Ehrlich, J.Y. Fu, A.A. Heikal, S.E. Hess, T. Kogej, M.D. Levin, S.R. Marder, D. McCord-Maughon, J.W. Perry, H. Rockel, M. Rumi, C. Subramaniam, W.W. Webb, X.L. Wu, C. Xu, Design of organic molecules with large two-photon absorption cross sections, Science 281 (1998) 1653–1656;
(b) M. Pawlicki, H.A. Collins, R.G. Denning, H.L. Anderson, Two-photon absorption and the design of two-photon dyes, Angew. Chem. Int. 48 (2009) 3244–3266.
[9] (a) F. Terenziani, C. Katan, E. Badaeva, S. Tretiak, M. Blanchard-Desce, Enhanced two-photon absorption of organic chromophores: theoretical and experimental assessments, Adv. Mater. 20 (2008) 4641–4678;
(b) K. Ohta, S. Yamada, K. Kamada, A.D. Slepkov, F.A. Hegmann, R.R. Tykwinski, L.D. Shirtcliff, M.M. Haley, P. Salek, F. Gel'mukhanov, H. Agren, Two-photon absorption properties of two-dimensional π-conjugated chromophores: combined experimental and theoretical study, J. Phys. Chem. 115 (2011) 105–117.
[10] (a) P. Wei, J.H. Oh, G.F. Dong, Z.N. Bao, Use of a ^{1}H-benzoimidazole derivative as an n-Type dopant and to enable air-stable solution-processed n-Channel organic thin-film transistors, J. Am. Chem. Soc. 132 (2010) 8852–8853;
(b) Y.M. Chen, W.-Y. Hung, H.W. You, A. Chaskar, H.C. Ting, H.-F. Chen, K.-T. Wong, Y.-H. Liu, Carbazole–benzimidazole hybrid bipolar host materials for highly efficient green and blue phosphorescent OLEDs, J. Mater. Chem. 21 (2011) 14971–14978;
(c) M.-Y. Lai, C.-H. Chen, W.-S. Huang, J.T. Lin, T.-H. Ke, L.-Y. Chen, M.-H. Tsai, C.-C. Wu, Benzimidazole/amine-based compounds capable of ambipolar transport for application in single-layer blue-emitting OLEDs and as hosts for phosphorescent emitters, Angew. Chem. Int. Ed. 47 (2008) 581–585;
(d) G.Y. Chen, S.C. Lan, P.Y. Lin, C.W. Chu, K.H. Wei, synthesis and characterization of a thiadiazole/benzoimidazole-based copolymer for solar cell applications, J. Polym. Sci. A: Polym. Chem. 48 (2010) 4456–4464.
[11] (a) Z.Y. Ge, T. Hayakawa, S. Ando, M. Ueda, T. Akiike, H. Miyamoto, T. Kajita, M. Kakimoto, Solution-processable bipolar triphenylamine–benzimidazole derivatives for highly efficient single-layer organic light-emitting diodes, Chem. Mater. 20 (2008) 2532–2537;
(b) Z.Y. Ge, T. Hayakawa, S. Ando, M. Ueda, T. Akiike, H. Miyamoto, T. Kajita, M. Kakimoto, Spin-coated highly efficient phosphorescent organic light-emitting diodes based on bipolar triphenylamine–benzimidazole derivatives, Adv. Funct. Mater. 18 (2008) 584–590.
[12] (a) P. Wei, X.D. Bi, Z. Wu, Z. Xu, Synthesis of triphenylamine-cored dendritic two-photon absorbing chromophores, Org. Lett. 7 (2005) 3199–3202;
(b) F. Terenziani, C. Le Droumaguet, C. Katan, O. Monginn, M. Blanchard-Desce, Effect of branching on two-photon absorption in triphenylbenzene derivatives, ChemPhysChem 8 (2007) 723–734;
(c) W. Huang, F.S. Tang, B. Li, J.H. Su, H. Tian, Large D–π–A–π–D structure with cyano- and triazine-substituted for efficient AIEE solid emitters and large two-photon absorption cross sections, J. Mater. Chem. C (2013), http://dx.doi.org/10.1039/C3TC31913J;
(d) S.M. Zeng, X.H. Ouyang, H.P. Zeng, W. Ji, Z.Y. Ge, Synthesis, tunable two and three-photon absorption properties of triazine derivatives by branches, Dyes Pigm. 94 (2012) 290–295.
[13] Q. Zhang, Z. Ning, H. Tian, 'Click' synthesis of starburst triphenylamine as potential emitting material, Dyes Pigm. 81 (2009) 80–84.
[14] (a) B. Gu, W. Ji, P.S. Patil, S.M. Dharmaprakash, H.T. Wang, Two-photon-induced excited-state absorption: theory and experiment, Appl. Phys. Lett. 92 (2008) 091118;
(b) B. Gu, W. Ji, Two-step four-photon absorption, Opt. Express 16 (2008) 10208–10213;
(c) N. Venkatram, R. Sathyavathi, D.N. Rao, Size dependent multiphoton absorption and refraction of CdSe nanoparticles, Opt. Express 15 (2007) 12258–12263.
[15] H.M. Kim, M.S. Seo, S.-J. Jeon, B.R. Cho, Two-photon absorption properties of hexa-substituted benzene derivatives: comparison between dipolar and octupolar molecules, Chem. Commun. (2009) 7422–7424.
[16] (a) Z.R. Grabowski, K. Rotkiewicz, W. Rettig, Structural changes accompanying intramolecular electron transfer: focus on twisted intramolecular charge-transfer states and structures, Chem. Rev. 103 (2003) 3899–4031;
(b) Q. Zhang, T. Komino, S. Huang, S. Matsunami, K. Goushi, C. Adachi, Triplet exciton confinement in green organic light-emitting diodes containing luminescent charge-transfer Cu(I) complexes, Adv. Funct. Mater. 22 (2012) 2327–2336.
[17] (a) W.J. Li, D.D. Liu, F.Z. Shen, D.G. Ma, Z.M. Wang, T. Feng, Y.X. Xu, B. Yang, Y.G. Ma, A twisting donor-acceptor molecule with an intercrossed excited state for highly efficient, deep-blue electroluminescence, Adv. Funct. Mater. 22 (2012) 2797–2803;
(b) X. Feng, J.-Y. Hu, H. Tomiyasu, N. Seto, C. Redshaw, M.R.J. Elsegoodd, T. Yamato, Synthesis and photophysical properties of novel butterfly-shaped blue emitters based on pyrene, Org. Biomol. Chem. 11 (2013) 8366–8374.
[18] (a) S.T. Zhang, W.J. Li, L. Yao, Y.Y. Pan, F.Z. Shen, R. Xiao, B. Yang, Y.G. Ma, Enhanced proportion of radiative excitons in non-doped electro-fluorescence generated from an imidazole derivative with an orthogonal donor–acceptor structure, Chem. Commun. 49 (2013) 11302–11304;
(b) X.H. Ouyang, X.Y. Zhang, Z.Y. Ge, Enhanced efficiency in nondoped, blue organic light-emitting diodes utilizing simultaneously local exciton and two charge-transfer exciton from benzimidazole-based donor-acceptor molecules, Dyes Pigm. 103 (2014) 39–49.
[19] N.S. Makarov, M. Drobizhev, A. Rebane, Two-photon absorption standards in the 550–1600 nm excitation wavelength range, Opt. Express 16 (2008) 4029–4047.
[20] G. Argouarch, R. Veillard, T. Roisnel, A. Amar, H. Meghezzi, A. Boucekkine, V. Hugues, O. Mongin, M. Blanchard-Desce, F. Paul, Triaryl-1,3,5-triazinane-2,4,6-triones (isocyanurates) peripherally functionalized by donor groups: synthesis and study of their linear and nonlinear optical properties, Chem. Eur. J. 18 (2012) 11811–11827.
[21] C.Y. Nie, Q. Zhang, H.J. Ding, B. Huang, X.Y. Wang, X.H. Zhao, S.L. Li, H.P. Zhou, J.Y. Wu, Y.P. Tian, Two novel six-coordinated cadmium(II) and zinc(II) complexes from carbazate β-diketonate: crystal structures, enhanced two-photon absorption and biological imaging application, Dalton Trans. 43 (2014) 599–608.
[22] H. Yilmaz, B. Kucukoz, G. Sevinc, S. Tekin, H.G. Yaglioglu, M. Hayvali, A. Elmali, The effect of charge transfer on the ultrafast and two-photon absorption properties of newly synthesized boron-dipyrromethene compounds, Dyes Pigm. 99 (2013) 979–985.